

Magnetic Divertors

M. Keilhacker

IPP III/33

November 1976



MAX-PLANCK-INSTITUT FÜR PLASMAPHYSIK

8046 GARCHING BEI MÜNCHEN

MAX-PLANCK-INSTITUT FÜR PLASMAPHYSIK
GARCHING BEI MÜNCHEN

Magnetic Divertors

M. Keilhacker

IPP III/33

November 1976

Paper presented at Summer School on
"Tokamak Reactors for Breakeven",
Erice, September 1976.

*Die nachstehende Arbeit wurde im Rahmen des Vertrages zwischen dem
Max-Planck-Institut für Plasmaphysik und der Europäischen Atomgemeinschaft über die
Zusammenarbeit auf dem Gebiete der Plasmaphysik durchgeführt.*

Magnetic Divertors

M. Keilhacker

Max-Planck-Institut für Plasmaphysik, Garching, Germany

ABSTRACT

The different needs for divertors in large magnetic confinement experiments and prospective fusion reactors are summarized, special emphasis being placed on the problem of impurities. After alternative concepts for reducing the impurity level are touched on, the basic principle and the different types of divertors are described. The various processes in the scrape-off and divertor regions are discussed in greater detail. The dependence of the effectiveness of the divertor on these processes is illustrated from the examples of an ASDEX/PDX-size and a reactor-size tokamak. Various features determining the design of a divertor are dealt with. Among the physical requirements are the stability of the plasma column and divertor throat and the problems relating to the start-up phase. On the engineering side, there are requirements on the pumping speed and energy deposition, and for a reactor, the need for superconducting coils, neutron shields and remote disassembly.

I. INTRODUCTION

It was as long as 25 years ago that Professor Lyman Spitzer at Princeton described and proposed the concept of a magnetic divertor /1/: a coil configuration that magnetically diverts an outer layer of the magnetic flux confining the plasma and conducts this flux - and with it the surface plasma - to an external chamber. This concept was then tested experimentally on the B-65 Stellarator in 1957 and on the Model C Stellarator in 1963, where it proved to be very effective, reducing impurities by an order of magnitude and decreasing the recycling.

Despite this successful operation no further divertor experiments were proposed until a few years ago when the attempt to reach the collisionless plasma regime in high-power-level tokamaks such as T-4 and TFR failed owing to an increased evolution of impurities. In addition, in these machines high-current discharges sometimes even damaged limiters and walls of the vacuum chamber. One of the most promising solutions to these problems appears to be the magnetic divertor. In a divertor the plasma boundary is defined by a magnetic limiter (separatrix) and contact with material walls is removed to a separate chamber. The divertor reduces contamination of the confined plasma by cutting down the recycling of cold gas (unloading action) and - under certain conditions - by screening off the influx of impurities from the vacuum chamber wall (shielding action). Furthermore, the divertor is suited to solve the following additional problems related to a fusion reactor: to pump the particle throughput of 10^{22} - 10^{23} particles/sec, to take up the energy flux of several 100 MW associated with this particle through-put, and to remove fuel (D, T) and ash (He).

In the following discussion of magnetic divertors emphasis is more on the physical aspects of a divertor than on its engineering problems. The paper starts by outlining the needs and possible methods of impurity control (section 2). Then the basic principle of a divertor, the stability requirements on the divertor field configuration and problems relating to the start-up of the plasma current are described (section 3). The main part of the paper (section 4) deals with the various processes in the scrape-off and divertor regions that determine the effectiveness of a divertor. Section 5 finally discusses engineering requirements of a divertor.

II. SIGNIFICANCE OF IMPURITIES IN LARGE FUSION EXPERIMENTS

II. 1. Need for Impurity Control

Impurities have a number of deleterious effects on large magnetic confinement experiments and prospective fusion re-

actors. These effects have already been widely discussed (e.g. /2/ - /6/) and will only be briefly summarized here:

- i) Enhanced radiation losses due to line radiation (partially stripped impurities) and recombination and bremsstrahlung radiation (fully stripped impurities).
- ii) Changes in temperature and current profiles: Edge cooling by low-Z impurities may cause the plasma to shrink and become unstable to a disruption, while high-Z impurities near the plasma centre may cause hollow temperature profiles and unstable current.
- iii) Reduction of reacting fuel ion density resulting in a decrease of thermonuclear reaction rates and an increase in ignition temperature.
- iv) Reduced neutral beam penetration ($\zeta_{i,eff} \approx Z_{eff} \zeta_{i,i}$) leading to increased requirements on beam energy.

Apart from their role in present-day and next-generation tokamak experiments impurities severely affect the economy of prospective fusion reactors. Especially the presence of high-Z impurities, because of the afore-mentioned processes i) and iii), shifts the Lawson and ignition criteria significantly towards higher temperatures and finally rules out ignition altogether. A number of studies /4,5/ have indicated that the maximum tolerable impurity concentrations, above which ignition is no longer possible, are 5 to 10 % for low-Z (C,O), 0.5 to 1 % for medium-Z (Fe to Mo) and about 0.1 % for high-Z (W, Au, Ta) impurities. This is illustrated in Fig.1.

II. 2. Origin of Impurities

During the steady-state phase of conventional tokamak discharges impurities are mainly produced by the following processes:

- i) Charged particle sputtering (hydrogen and impurity ions) of the vacuum chamber wall and limiters
- ii) Neutral particle sputtering (fast charge-exchange atoms) of the vacuum chamber wall

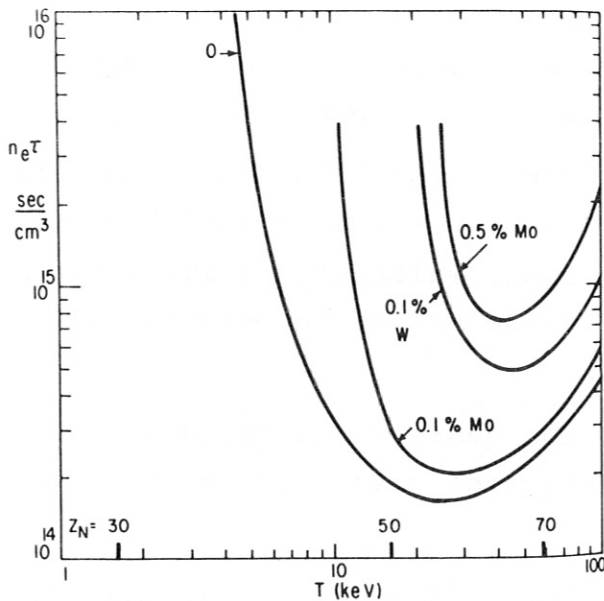


Fig.1: Ignition condition for D-T, with various percentages of molybdenum and tungsten impurity contamination /4/. The vertical bars indicate the temperatures at which ions of nuclear charge Z_N are ionized to helium-like states.

- iii) Evaporation of limiter or wall material due to overheating.
- iv) Desorption from the wall surface by ions, electrons or photons.

Prior to the quasi-stationary phase with constant plasma current, impurities are generated during the initial phase of plasma breakdown and plasma current build-up. During this period there is special danger of plasma-wall contact and of evaporation by run-away electrons.

II. 3. Possible Methods of Impurity Control

Various methods have been proposed to control the impurity concentration of the plasma. These methods may be divided into three groups depending on the point at which the process of plasma contamination is interrupted:

- i) Methods to suppress the sputtering and thus the formation of impurities itself

ii) Methods to shield the hot plasma core against the influx of impurities

iii) Methods to retard or even reverse the accumulation of impurities in the centre of the plasma (purification).

i) The most obvious method to suppress sputtering seems to be the use of special wall material resistant to sputtering. In addition, charge-exchange sputtering of the wall material can be strongly reduced if the temperature of the plasma edge is kept low, either by radiation cooling or by injecting hydrogen gas. The first method could be used in a controlled way by making walls and limiter out of suitable low-Z material. In the second case - injection of hydrogen gas - a cold, dense outer plasma region is formed that protects, at least transiently, the wall from charge-exchange-neutral bombardment while, at the same time shielding the hot plasma core against the influx of cold neutral gas and impurities. To get this favourable effect on the sputtering problem, it must be ensured that the mean energy of the resultant charge-exchange neutrals stays below the sputtering threshold of the wall material. This concept of a cold-gas (cold-plasma) blanket has been proposed by H. Alfvén and E. Smårs /7/ and is discussed, e.g. in ref./7-10/. A viable solution to this problem, of course, is a magnetic divertor, reducing both the plasma ion and charge-exchange neutral sputtering, as will be discussed later.

ii) The influx of sputtered impurity atoms can be attenuated in the outer plasma layer by a magnetic divertor or possibly by a cold gas blanket. In the divertor, part of the incoming impurity atoms are ionized in the scrape-off layer and swept into the divertor by the outflowing plasma. In the case of a continuously refreshed cold gas blanket impurities could be flushed away with the outstreaming gas.

iii) The most important, but least understood, problem is how to retard or possibly reverse the inward diffusion of impurities

predicted by classical theory. Several techniques have been proposed to give the impurities an outward momentum, e.g. the use of plasma waves /11,12/ or local injection of hydrogen gas /13/. Also, if the impurity transport is classical, the impurities could be forced to flow outward by reversing the hydrogen plasma density gradient towards the plasma edge either by neutral beam injection ("profile shaping") or by means of a cold-plasma blanket.

III. DIVERTOR MAGNETIC FIELD CONFIGURATION

III. 1. Basic Principle and Types of Divertors

The principle of the magnetic divertor is well known and shall only be briefly described here as a basis for the following discussion.

External currents near the plasma surface produce a separatrix that defines the size and shape of the hot plasma. Charged particles diffusing across this separatrix can flow along the magnetic field lines into a separate chamber where they are neutralized at collector plates and can be pumped off. This removal of the cold neutral reflux (the recycling) reduces charge-exchange sputtering of the vacuum chamber walls.

The plasma region outside the separatrix, lying on magnetic field lines that enter the divertor, is called the scrape-off layer. If this layer is sufficiently thick and dense, it can shield the hot plasma against wall-originated impurity atoms: the incoming impurity atoms become ionized and are then swept into the divertor by the outflowing plasma.

There are various types of divertors. They may be divided into two groups depending on whether the toroidal or poloidal field is distorted: toroidal divertors (Model C Stellarator, 1964) and poloidal divertors (FM-1, 1973; DIVA, 1974; PDX, 1978; ASDEX, 1978). The latter are also called axisymmetric

divertors since they preserve the axisymmetry of the tokamak. A special kind of toroidal divertor is the bundle divertor where only a small part of the toroidal flux is diverted (DITE, 1975; proposed for TEXTOR).

III. 2. Stability of Divertor Field Configurations

One of the most important criteria for choosing a particular divertor field configuration is its MHD stability. This question has therefore been investigated intensively during the last years at different laboratories (see, for example, ref. /14/ and references cited therein). Here only the most pertinent results related to poloidal (axisymmetric) divertors can be summarized in a more qualitative fashion:

i) The divertor fields have to be localized, i.e. of short range, in order not to affect the equilibrium, stability and shape of the plasma. This rules out arrangements in which the divertor field is produced by a single coil carrying current parallel to the plasma current (Fig. 2a or, equivalently, Fig. 2b), and calls for divertor coil triplets with zero net current (Fig. 2c,d). More specifically, the results of hexapole and octupole calculations presented in ref. /14/ show that the stability against axisymmetric modes is the better the more localized the divertor field is, thus probably ruling out a hexapole configuration.

ii) Divertor configurations where the plasma cross-section is "D"-shaped (Fig. 2c) are stable over a wider range of plasma parameters than those with an "inverse D" (Fig. 2d).

iii) As far as the shape of the plasma cross-section is concerned for axisymmetric modes the stability is best for a circular cross-section, while for non-axisymmetric modes a triangular deformation of the plasma cross-section tends to improve the stability.

Apart from the MHD stability of the plasma column, the following points have to be considered in designing a divertor

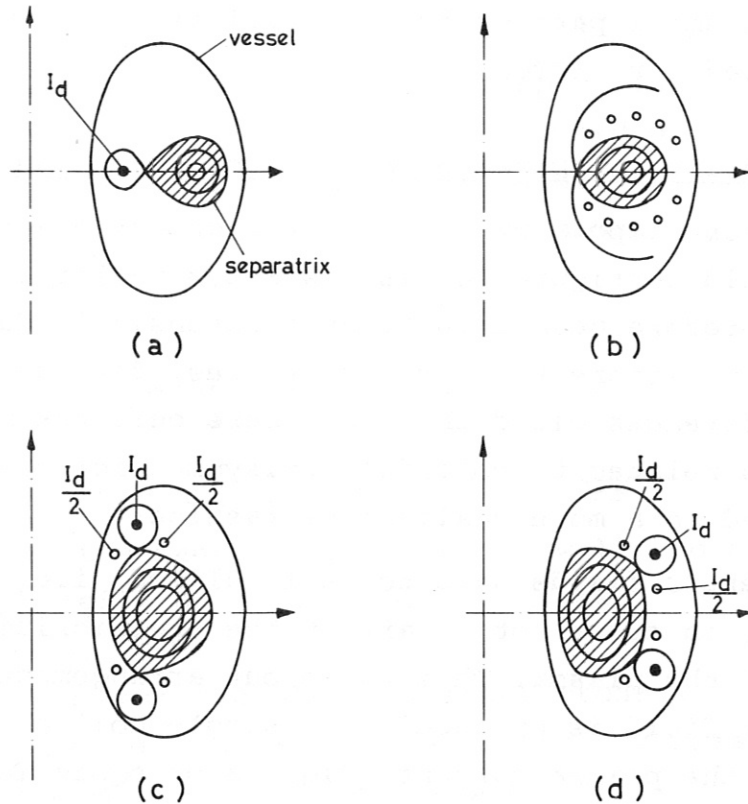


Fig. 2: Various axisymmetric divertor configurations with parallel (•) and antiparallel (○) currents

field configuration: positional stability of the scrape-off layer in the divertor throat, plasma breakdown near the centre of the vacuum chamber, possibility of an expanding magnetic limiter without programmed divertor currents (see following paragraph).

III. 3. Expanding Magnetic Limiter for Controlling the Skin Effect

The turbulence associated with the skin effect during the current-rise phase in large tokamaks is expected to transfer a large amount of energy to the walls and limiter, thereby boiling off impurities. To suppress this skin effect, one

would like to enforce proportionality between the plasma cross-section and the plasma current.

In a divertor tokamak this is possible by having the separatrix expand in a controlled way with the rising plasma current. In practice, however, it is not possible to enforce this perfect magnetic limiter behaviour over a large range of plasma currents by simply varying the currents in the divertor coils. An elegant way out of this difficulty, proposed by K. Lackner and discussed in refs. /15/ and /17/, is not to vary the divertor currents but rather to shift the plasma column ("plasma displacement limiter") by proper magnetic fields into the vicinity of one of the divertor stagnation points and then to let it come back to the median plane in a controlled way. This kind of expanding magnetic limiter has the further advantage that even during current build-up the plasma is connected to one of the divertors. Another concept for a plasma displacement limiter would be to strike the discharge near a mechanical limiter on the inside of the torus or at the centre of an octupole magnetic null /19/ and to let the plasma move radially outward in a controlled way as the current rises.

IV. DIVERTOR EFFECTIVENESS

IV. 1. Impurity Build-up with and without Divertor

The operation of a divertor system is specified mainly by the following three parameters:

- C , the plasma capture efficiency of the divertor; a large C reduces the plasma ion sputtering of the limiter
- R , the backstreaming ratio, i.e. the fraction of neutral gas that returns from the divertor into the vacuum chamber; a small R reduces the charge-exchange neutral sputtering
- P , the shielding efficiency of the scrape-off region; a large P prevents wall-originated impurities from reaching the hot plasma core.

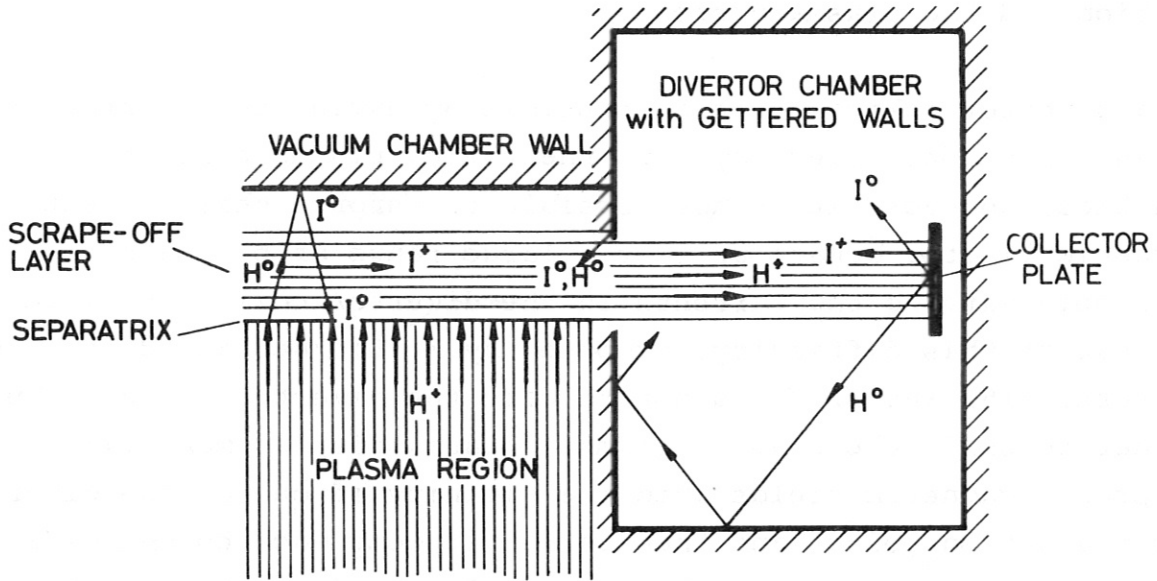


Fig. 3: Idealized representation of processes in the scrape-off and divertor regions

To see in how far a divertor is capable of reducing the level of impurities, we look at the build-up of impurities in a steady-state confined plasma due to charge-exchange and ion sputtering of the walls, limiter and collector plate as depicted in Fig. 3. In this simplified model, that neglects desorption, evaporation, blistering etc., the build-up of impurities can be described by the following relation:

$$\dot{n}_I + \frac{n_I}{\tau_I} = \frac{n}{\tau_p} \left\{ (1 - C) (S_{HL} + \gamma_H S_{HW}) (1 - P) + C \left[S_{HD} P_i (1 - P_d) + R \gamma_{H_2} S_{HW} (1 - P) \right] \right\} + \frac{n_I}{\tau_I} \left[(1 - C) S_{IL} (1 - P) + C S_{ID} P_i (1 - P_d) \right] \quad (1)$$

Here n and n_I denote the particle densities, τ_p and τ_I the confinement times of the hydrogen and impurity ions, respectively. S_{HL} , S_{HW} and S_{HD} are the sputtering coefficients for hydrogen bombardment of the limiter, the wall and the collector plate, S_{IL} and S_{ID} the corresponding coefficients for sputtering by impurities. P_i is the ionization probability of an impurity ion in the scrape-off layer or in the plasma layer in front of the collector plate (the area density of the plasma is assumed equal in these two regions), P_d the probability that an impurity ion in the scrape-off layer is swept into the divertor before it diffuses into the confined plasma. Consequently, the product of P_i and P_d is the shielding efficiency P as defined before. The coefficients γ give the number of fast charge-exchange neutrals that result per neutralized plasma ion.

The first line of equ. (1) describes the build-up of impurities caused by that part of the plasma that impinges on the edges of the divertor slits (which in this case are equivalent to the limiter). The second line represents the contribution by the plasma that enters the divertor and sputters the collector plate. A fraction P_i of the sputtered material becomes ionized and enters the vacuum chamber along the magnetic field lines. Of the neutralized gas a part R flows back into the vacuum chamber and leads to charge-exchange sputtering. The third line of equ. (1) finally describes the contamination due to sputtering by the impurity ions that are lost from the confined plasma.

For a qualitative discussion of divertor effectiveness one can simplify equ. (1). First, in a working divertor sputtering by impurities can be neglected. Furthermore we confine the discussion to a divertor of the unload type, i.e. with $C \approx 1$.

This leads to the following expression for the build-up of impurities in an unload divertor (with $n_I = 0$ at $t = 0$):

$$\frac{n_I}{n} = \mathcal{D} \frac{\tau_I}{\tau_p} \left[1 - \exp(-t/\tau_I) \right] \quad (2)$$

$$\text{with } \mathcal{D} = S_{HD} P_i (1 - P_d) + R \gamma_{H_2} S_{HW} (1 - P) .$$

The build-up of impurities reaches a stationary state after a time of the order of the impurity confinement time τ_I . The absolute value of this stationary impurity concentration $C_{I, st} = n_{I, st}/n \approx D \tau_I / \tau_p$ depends mainly on P_i and R and will typically be between 10^{-3} and 10^{-2} (for $\tau_I = \tau_p$).

For long impurity confinement times (for $\tau_I \gg \tau_p, t$) one obtains from equ. (2):

$$\frac{n_I}{n} = D \frac{t}{\tau_p}, \quad (3)$$

i.e. the number of impurities increases linearly with time.

Let us now, for comparison, look at the build-up of impurities in a tokamak without divertor. In this case one gets from equ. (1) (with $C = 0, P = 0$):

$$\frac{n_I}{n} = \frac{\mathcal{L}}{(1 - S_{IL})} \frac{\tau_I}{\tau_p} \left[1 - \exp - (1 - S_{IL}) t / \tau_I \right] \quad (4)$$

$$\text{with } \mathcal{L} = S_{HL} + \nu_H S_{HW},$$

i.e. the impurities build up exponentially without saturation if the sputtering coefficient of the impurities, S_{IL} , is larger than 1 (this may well be the case, unless the temperature of the sputtering impurities stays rather low, say below 500 eV).

For $\tau_I \gg \tau_p, t$ one gets by analogy with equ. (3)

$$\frac{n_I}{n} = \mathcal{L} \frac{t}{\tau_p}. \quad (5)$$

A comparison of the build-up of impurities with and without divertor shows that the impurity concentrations, $C_{I, st}$, that are reached in the stationary state (in the limiter case, of course, only for $S_{IL} < 1$) are related to each other by

$$\mathcal{R} = \frac{C_{I, \text{st Div}}}{C_{I, \text{st Lim}}} = \frac{D |1 - S_{IL}|}{\mathcal{L}} \quad (6)$$

To get a rough idea how this "figure of merit" for divertors, \mathcal{R} , depends on the main divertor characteristics, one may simplify the expression for \mathcal{R} by neglecting S_{HL} compared to $\gamma_H S_{HW}$ (this is usually justified) and by dropping the term $S_{HD} P_i (1 - P_d)$ (which has to be checked in each case). One then gets

$$\mathcal{R} = C R (1 - P) |1 - S_{IL}| \quad , \quad (7)$$

where C , which had been assumed to be about 1, is included again for the sake of greater generality and γ_H was assumed equal to γ_{H_2} .

Since it is not possible to design a divertor in which C , R and P are all optimized at the same time, one mainly has two modes of operation for a divertor system: an unload divertor ($C \approx 1$, $R \approx 0$, $P \approx 0$) or a shielding divertor ($C \approx 1$, $0 \ll R \ll 1$, $P \approx 1$).

IV. 2. The Processes that Determine the Divertor Effectiveness

a) Density Profile in the Scrape-off Layer

To determine the density profile in the scrape-off region, one may consider a simple one-dimensional model /16, 18-20/ in which plasma diffusion across the magnetic field (diffusion coefficient $D_{\perp s}$) is balanced by plasma loss parallel to the field lines into the divertor (effective confinement time τ_{\parallel}). Neglecting ionization in the scrape-off region is justified for a working divertor.

If x is the distance across the scrape-off layer, one has

$$\frac{d}{dx} (D_{\perp s} \frac{dn}{dx}) = \frac{n}{\tau_{\parallel}} \quad (8)$$

Assuming $D_{\perp s}$ and τ_{\parallel} are constant across the scrape-off region (for τ_{\parallel} this is strictly speaking only correct for a divertor of the C-Stellarator type), the density profile is given by

$$n = n_b \exp(-x/\Delta_d), \quad (9)$$

where
$$\Delta_d = (D_{\perp s} \tau_{\parallel})^{1/2} \quad (10)$$

is the width of the scrape-off region.

The boundary density n_b is determined by the condition that the total plasma flow across the separatrix ($x=0$) has to equal the total loss of confined plasma:

$$-A_p D_{\perp s} \left. \frac{dn}{dx} \right|_{x=0} = \frac{\bar{n} V_p}{\tau_p},$$

\bar{n} , A_p and V_p being the average density, surface and volume of the confined plasma, respectively. This then yields for the boundary density

$$n_b = \frac{\bar{n} a}{2 \tau_p} \cdot \frac{\Delta}{D_{\perp s}} \quad (11)$$

where a is the plasma radius.

For divertors with no magnetic mirrors, i.e. with stagnation lines on the outside of the plasma column, the plasma in the scrape-off region flows into the divertor with ion sound speed, v_s ("ion sound model"), i.e. τ_{\parallel} is simply given by $\tau_{\parallel} = L/v_s$, where L is the geometrical path length into the divertor.

The situation is different if the stagnation lines lie on the inside of the plasma core, and the plasma in the scrape-off layer therefore encounters a mirror on its way into the divertor. In this case the scrape-off region may be mostly populated by trapped particles and the plasma flows into the divertor by scattering into the mirror loss cone ("mirror confinement model"). The effective confinement time of the plasma in the scrape-off region is then approximately equal to the scattering time of trapped particles into the loss cone, τ_{sc} , since one can show that for most divertors $\tau_{sc} > L/v_s$. In the

mirror model one thus has

$$\tau_{\parallel} \approx \tau_{90^{\circ}} \log_{10} M$$

where $\tau_{90^{\circ}}$ is the 90° scattering time for ions in the scrape-off region and M is the mirror ratio.

Since in the mirror model τ_{\parallel} depends on the density n , the solution of equ.(8) is slightly different from that for the ion sound model. Assuming $D_{\perp s}$ and the temperature T to be constant across the scrape-off layer the density profile in the mirror model is

$$n = n_b^* \left(1 + \frac{x}{\Delta_d^*}\right)^{-2} \quad (12)$$

with
$$n_b^* = \frac{\bar{n} a}{4 \tau_p} \frac{\Delta_d^*}{D_{\perp s}} \quad (13)$$

and
$$\Delta_d^{*3} = 3.4 \times 10^8 \frac{A^{1/2} T(\text{eV})^{3/2} \tau_p D_{\perp s}^2 \log_{10} M}{\bar{n} a \ln \Lambda} \quad (14)$$

In calculating Δ_d^* the value given by Spitzer /21/ was used for $\tau_{90^{\circ}}$ and n_b^* was expressed by \bar{n} by means of equ.(13).

The diffusion width of the scrape-off layer Δ_d (or Δ_d^*), as calculated above, is only meaningful as long as it is larger than the excursions Δ_b which the ions undergo on their path to the divertor. If, on the other hand, $\Delta_d < \Delta_b$ then the width of the scrape-off layer is determined by Δ_b . The order of magnitude of this so-called banana width is given by

$$\Delta_b \approx \sqrt{\frac{a}{R}} r_{ip},$$

where r_{ip} is the ion gyro-radius in the poloidal field.

For divertor experiments like ASDEX and PDX the banana width Δ_b is comparable to the diffusion width Δ_d (no mirrors) but smaller than Δ_d^* (with mirrors). In a divertor for a reactor the diffusion width Δ_d should prevail in any case (c.f. Table I).

b) Plasma Capture Efficiency of the Divertor

The plasma capture efficiency of the divertor is

$$C = 1 - \exp (- W / \Delta') ,$$

where W is the width of the divertor throat and Δ' the characteristic length of the density drop in the scrape-off layer projected into the divertor throat, i.e. $\Delta' = (B_p / B'_p) \Delta$, where B'_p is the poloidal field in the divertor throat and B_p is the average poloidal field. For Δ the diffusion width Δ_d or the banana width Δ_b has to be taken, whichever is larger. For $W / \Delta' = 4$, for example, a value that is easily attainable in most divertor designs, one gets $C \approx 0.98$, i.e. most of the outstreaming plasma goes into the divertor.

c) Neutral Gas Return from the Divertor

As discussed before, efficient divertor operation requires that only a small fraction of the neutral gas that is generated in the divertor by neutralizing the incoming plasma should return to the main confinement chamber. The large pumping speeds required for this purpose (e.g. 6×10^6 l/s in ASDEX /22/) can only be achieved by getter pumps. The getter pumping may be supplemented by trapping of plasma ions in the collector plates and by plasma pumping in the divertor throats (plasma pumping constitutes about 10 - 20 % of the total pumping in PDX and ASDEX).

Neglecting plasma pumping, the fraction of neutral gas that returns from the divertor is given by

$$R = \frac{L (1 - f_p)}{L + S} ,$$

where L is the conductance of the divertor throat, f_p the trapping efficiency of the collector plates for plasma ions, and $S = f_n A$ the pumping speed (f_n is the intrinsic pumping speed, A the area of the gettering surface, respectively).

d) Shielding Efficiency of the Scrape-off Layer

The shielding process in the scrape-off layer consists of two steps: first the incoming wall-impurity atom has to be ionized and then the ion has to be swept into the divertor. In order to shield the plasma core effectively, the ionization process has to take place so far away from the separatrix that the impurity ion cannot diffuse into the confined plasma during its flight into the divertor.

Let us first consider the ionization process /2,16,18,19,20,23/. The penetration of impurity atoms into the scrape-off region is given by

$$v_{oI} \frac{dn_I}{dx} = -n_I n \langle \zeta v \rangle_i, \quad (15)$$

where n_I , v_{oI} and $\langle \zeta v \rangle_i$ are the density, radial velocity and ionization rate of the incoming impurity atoms.

The solution of this equation

$$n_I(x) = n_I(\infty) \exp \left[- \frac{\langle \zeta v \rangle_i}{v_{oI}} \int_0^\infty n dx \right] \quad (16)$$

can be used to calculate the fraction of incoming impurities that are ionized within the scrape-off layer (up to the separatrix at $x=0$)

$$P_i = 1 - \frac{n_I(0)}{n_I(\infty)} = 1 - \exp \left[- \frac{\langle \zeta v \rangle_i}{v_{oI}} \int_0^\infty n dx \right]. \quad (17)$$

The ionization probability, P_i , thus depends only on the area density of the scrape-off layer, $\int_0^\infty n dx$. For a given area density the ionization probability becomes larger for heavier impurities since $v_{oI} \propto (kT_I/A)^{1/2}$ and since one can assume that the impurity atoms all come off the wall with the same mean energy kT_I (c.f. the values for P_i (16) and P_i (100) in Table I).

The area density can be evaluated by using the density profiles given by equs. (9) and (12) (which yield $n_b \Delta_d$ and $n_b \Delta_d^*$, respectively) or by making use of the relation

$$\int_0^{\infty} n dx = \frac{\bar{n} a}{2 \tau_p} \tau_{||} \quad (18)$$

where $\tau_{||}$ is again the effective confinement time of the plasma in the scrape-off region.

Relation (18) shows that in order to improve the ionization probability and by this the screening efficiency, one has to increase the confinement time of the plasma in the scrape-off region $\tau_{||}$. Now $\tau_{||}$ can either be extended by increasing the geometrical path length into the divertor, L (torsatron, bundle divertor) or by having a magnetic mirror in the divertor throat (inside poloidal divertor, bundle divertor).

By increasing L , however, one also increases the confinement time of the impurity ions in the scrape-off region, $\tau_{||I}$, and therefore their inward diffusion distance

$$d = (D_{\perp s, I} \tau_{||I})^{1/2} \quad \text{with } \tau_{||I} = L/v_{||I},$$

where $D_{\perp s, I}$ and $v_{||I}$ are the diffusion coefficient and parallel flow velocity of the impurity ions in the scrape-off region. In the case that the width of the scrape-off layer, Δ , is determined by diffusion (and therefore has the same dependence on L) one gets

$$\frac{d}{\Delta} = \frac{D_{\perp s, I} v_s}{D_{\perp s} v_{||I}}$$

i.e. the inward diffusion distance of the impurity atoms is a fixed fraction of the scrape-off width, irrespective of the geometrical path length.

Let us now consider the case in which the confinement time of the plasma in the scrape-off region is increased by a magnetic mirror in the divertor throat. In contrast to the geometrical path length, on which the confinement times of both plasma and impurity ions depend in the same way, the effect of magnetic mirrors is different for the plasma and the impurity ions. This is because the impurity ions in the scrape-off region are swept into the divertor by the plasma flow, either due to friction or due to an extended sheath potential $U_s = kT_e/e$. Since the impurities typically become highly ionized, but not heated much, during their transit time into the divertor their parallel velocity $v_{\parallel I} \approx (Z_I kT_e/m_I)^{1/2}$ is much larger than their perpendicular velocity $v_{\perp I} = (kT_I/m_I)^{1/2}$ and they therefore pass easily through the magnetic mirror. For the protons, however, $v_{\parallel} \approx v_{\perp}$ and they are trapped between the mirrors unless velocity-space instabilities enhance their parallel loss rate. Thus with a magnetic mirror it may be possible to increase the ionization probability for impurity atoms without impairing their parallel transport into the divertor.

e) Shielding Efficiency of Divertors for an ASDEX/PDX-Size and a Reactor-Size Tokamak

The width (Δ_b, Δ_d), plasma density (n_p) and shielding efficiency (P_i) of the scrape-off layer in the ion sound and the mirror confinement model, respectively, are illustrated for the examples of an ASDEX/PDX-size and an Experimental Power Reactor (EPR)-size tokamak in Table I. The following parameters have been used for the two reference tokamaks:

	a	R	B_t	\bar{n}	τ_p
	(cm)	(cm)	(KG)	(cm^{-3})	(sec)
PDX/ASDEX	40	150	30	3×10^{13}	0.05
EPR	200	600	60	6×10^{13}	2

$q(a)$ was assumed to be 3 and for L the relation $L \approx q(a) \pi R$ was used. The calculations were carried out for a deuterium plasma ($A=2$). The mirror ratio M was set equal to 2. Furthermore, the diffusion coefficient of the plasma in the scrape-off layer, $D_{\perp s}$, was assumed to be 1/10 of the Bohm-diffusion coefficient.

For the electron and ion temperatures in the scrape-off region two different values, 100 eV and 1000 eV, were used. The impurities were assumed to come off the wall with a velocity corresponding to 1 eV. For the ionization rate $\langle \Sigma v \rangle_i$, which is rather independent of temperature in the considered range of 10^2 to 10^3 eV, a value of $1 \times 10^{-7} \text{ cm}^3/\text{s}$ was used for light elements (C, O, CO) and of $3 \times 10^{-7} \text{ cm}^3/\text{s}$ for heavy elements (Nb, Mo, W) /24/.

		Δ_b	Δ_d	n_b	$\int_0^{\infty} n dx$	$P_i(16)$	$P_i(100)$
		(cm)	(cm)	(10^{12} cm^{-3})	(10^{12} cm^{-2})		
<u>ION SOUND MODEL</u>							
ASDEX	100 eV	0.3	0.7	3.9	2.6	0.65	1
PDX	1000 eV	0.9	1.2	0.7	0.8	0.27	0.91
EPR	100 eV	0.1	0.9	2.7	2.6	0.65	1
	1000 eV	0.4	1.7	0.5	0.8	0.27	0.91
<u>MIRROR MODEL</u>							
ASDEX	100 eV	0.3	1.2	3.5	4.2	0.81	1
PDX	1000 eV	0.9	17.6	5.1	90	1	1
EPR	100 eV	0.1	1.2	1.7	2.1	0.57	1
	1000 eV	0.4	17.6	2.5	44	1	1

Table I

The results shown in Table I explain themselves. Δ_d is always larger than Δ_b and was therefore used in calculating n_b and $\int n dx$. If the diffusion in the scrape-off layer is larger than 1/10 of Bohm-diffusion, the width of the scrape-off layer becomes larger and the density smaller.

The ionization probability in the scrape-off layer for light elements, denoted by $P_i(16)$ (for $A=16$), is around 0.5 for the ion sound cases and between 0.6 and 1 for mirror confinement, whereas the ionization probability for heavy elements, $P_i(100)$ (for $A=100$), is 1 or close to 1 for all cases. If the impurities come off the wall with an energy larger than the assumed 1 eV the ionization probabilities become smaller. It has further to be remembered that ionization of the impurity atoms is only the first step of the shielding process and that a considerable fraction of the impurity ions may diffuse across the separatrix before they reach the divertor throat.

f) Refuelling a Divertor Tokamak

For "stationary" operation a divertor tokamak has to be refuelled, i.e. the plasma that flows off into the divertor has to be replaced. In the case of an unload divertor ($C \approx 1$, $R \approx 0$, $P \approx 0$), the effectiveness of which depends on keeping the recycling as small as possible, the gas source has to be located deep within the plasma. A shielding divertor on the other hand can either be refuelled from inside the plasma like an unload divertor ($R \approx 0$) or from outside the plasma by operating it with surface recycling ($R \approx 1$).

Possible refuelling methods are

- pellet injection
- cluster injection
- neutral injection
- cold gas inlet.

All these refuelling methods, which supply gas or neutral par-

ticles that have to be ionized for absorption in the plasma, lead to additional sputtering of the vacuum chamber wall and therefore increase the build-up of impurities. This can be taken into account by adding to equ. (1) a term of the form

$$(1 - R) \frac{n}{\tau_p} \sum_m (\alpha_m \gamma_m) S_{HW} P.$$

Here α_m denotes the fraction that a special method (pellet injection, cluster injection etc.) contributes to the refuelling and γ_m is the corresponding number of wall bombardment events which occur by charge-exchange, incomplete absorption and so on for every hydrogen ion, that is finally added to the plasma.

For ASDEX a combination of cluster injection, neutral injection and cold gas inlet is envisaged for refuelling /25/. The contribution of these three refuelling methods to the contamination of the plasma by metal impurities is discussed in /26/.

V. ENGINEERING ASPECTS OF THE DIVERTOR

In discussing the engineering aspects of the divertor, one might distinguish between the general requirements for a divertor design and those especially related to a fusion reactor. Among the general requirements - connected with the considerations on divertor efficiency, plasma stability, and plasma start-up, as discussed in the previous sections - the most important are:

- i) A poloidal magnetic field configuration that ensures equilibrium and stability of the confined plasma.
- ii) A pumping system that provides the necessary pumping speed and is capable of taking up the particle throughput.
- iii) A design of the exhaust channel and collector plates that is capable of taking up the energy flux associated with the particle throughput.

In addition, for a reactor the following are required:

- iv) Superconducting divertor coils that are shielded against the neutron flux.
- v) A design that allow remote disassembly of all components.
- vi) A possibility to recover the tritium.

As far as divertor experiments of the next generation, such as PDX and ASDEX, are concerned, the engineering requirements resulting from i) - iii) can be solved, and have already been more or less. Here we shall therefore only mention some of the consequences and possible solutions related to divertor designs for a reactor. Most of these points are discussed in more detail in some of the theoretical studies of divertors for possible fusion reactors /27 - 30/, the most recent study being a conceptual design of a divertor for a tokamak EPR jointly carried out by scientists from Princeton and the Soviet Union /31/. Figure 4 shows a cross-sectional view of this tokamak EPR divertor design.

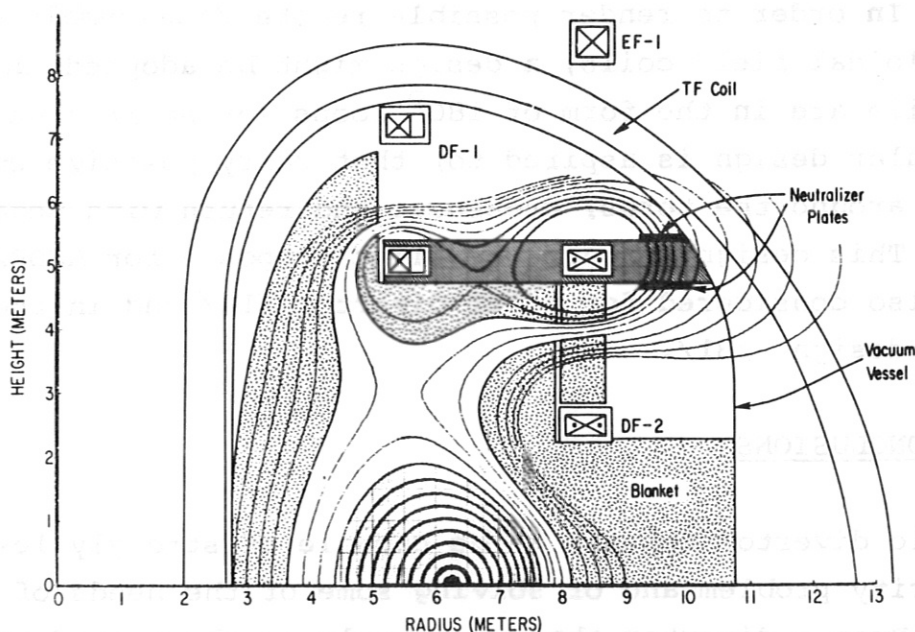


Fig.4: Cross-sectional view of the tokamak EPR divertor design of ref./31/ showing the toroidal field (TF) coil, divertor field (DF) coils and equilibrium field (EF) coil.

re ii) Since pumping speeds in the range of $10^7 - 10^8$ liters/sec are required, it becomes difficult to provide the necessary pumping area. A possible solution discussed in /31/ is to pump the escaping plasma at a higher velocity, e.g. 100 eV, instead of room temperature.

re iii) To take up the energy flux the scrape-off region in the divertor has to be spread out over a sufficiently large area of cooled neutralizer plates. The poloidal field in the divertor chamber should therefore form long "ears" to provide extended divertor exhaust channels. In this way, in the design of Fig.4, the power density on the neutralizer plate could be kept down to about 300 W/cm^2 (or even 150 W/cm^2 for a corrugated plate).

re iv) It might be mentioned that the concept of producing an expanding magnetic limiter by vertical displacement of the plasma column, as discussed in section III.3., is in accord with the use of superconducting divertor coils.

re v) In order to render possible remote disassembly of the inner poloidal field coils, a design might be adopted in which these coils are in the form of 180° loops (or shorter sections, if a modular design is aspired to) that carry positive current half-way around the torus, crossover and return with negative current. This design feature was first proposed for ASDEX /17/ and is also considered for a JET divertor /18/ and in the EPR divertor design /31/.

VI. CONCLUSIONS

A magnetic divertor appears to be capable of strongly lessening the impurity problem and of solving some of the needs of a fusion reactor. Even a divertor that works only in the unload mode ($C \approx 1$, $R \ll 0.1$, $P \approx 0$) should reduce the impurity level by about a factor of 10. Beyond that a divertor should be able to attenuate the influx of heavy metal impurities from the

wall. The shielding efficiency against light elements is more doubtful, since it depends mainly on mirror confinement of the plasma in the scrape-off region which might be impaired by loss-cone instabilities.

Alternative concepts for the control of impurities should therefore be pursued in parallel.

This work was performed under the terms of agreement on association between the Max-Planck-Institut für Plasmaphysik and EURATOM.

REFERENCES

- /1/ L. Spitzer, Jr., Report No. NYO-993, U.S. Atomic Energy Commission, Washington, D.C. (1951) and Phys. Fluids 1, 253 (1958)
- /2/ D. Düchs, G. Haas, D. Pfirsch, H. Vernickel, J. Nucl. Mat. 53, 102 (1974)
- /3/ E. Hinno, J. Nucl. Mat. 53, 9 (1974)
- /4/ D.M. Meade, Nucl. Fusion 14, 289 (1974)
- /5/ D. Eckhardt, E. Venus, JET Techn. Note 9 (1974)
- /6/ R. Behrisch, B.B. Kadomtsev, Plasma Physics and Controlled Nuclear Fusion Research, Vol. II, p.229, IAEA, Vienna (1975)
- /7/ H. Alfvén, E. Smårs, Nature 188, 801 (1960)
- /8/ C.M. Braams, Phys. Rev. Lett. 17, 470 (1966)
- /9/ B. Lehnert, Proc. 3rd Int. Symposium on Toroidal Plasma Confinement, Paper C1-I, Garching (1973)
- /10/ D.M. Meade, et al., Plasma Physics and Controlled Nuclear Fusion Research, Vol. I, p.621, IAEA, Vienna (1975)
- /11/ R. Dei-Cas, A. Samain, Plasma Physics and Controlled Nuclear Fusion Research, Vol. I, p.563, IAEA, Vienna (1975)
- /12/ T. Consoli, et al., Plasma Physics and Controlled Nuclear Fusion Research, Vol. I, p.571, IAEA, Vienna (1975)
- /13/ T. Ohkawa, General Atomic Report GA-A13017 (1974)
- /14/ G. Becker, K. Lackner, 6th International Conference on Plasma Physics and Controlled Nuclear Fusion Research, Berchtesgaden 1976, Paper B 11-3 (to be published)
- /15/ K.-U.v. Hagenow, K. Lackner, Bull. Am. Phys. Soc. 19, 852 (1974) and Proc. of 7th European Conf. on Controlled Fusion and Plasma Physics, Lausanne 1975, Vol. I, p.19

- /16/ ASDEX Proposal, Part I (October 1973)
- /17/ ASDEX Proposal, Part II (June 1974)
- /18/ The JET Project, First Proposal, Report EUR-JET-R2 (April 1974)
- /19/ PDX Official Planning Document, Special Report 74/2 (June 1974)
- /20/ A.M.Stefanovsky, Report IAEA-2540, Kurchatov-Institute, Moskow 1975
- /21/ L.Spitzer, Jr., Physics of Fully Ionized Gases, John Wiley & Sons, New York 1962
- /22/ R. Allgeyer et al., Proc. 6th Symposium on Engineering Problems of Fusion Research, San Diego 1975, p. 378
- /23/ A. Rogister, in Report on the Planning of TEXTOR (November 1975), p.B. II/4
- /24/ W. Lotz, IPP Report 1/62 (1967)
- /25/ G. Haas, W. Henkes, M. Keilhacker, R. Klingelhöfer, A. Stäbler, Proc. 6th Symposium on Plasma Heating in Toroidal Devices, Varenna 1976, in press
- /26/ G. Haas, M. Keilhacker, Proc. International Symposium on Plasma Wall Interaction, Jülich 1976, to be published
- /27/ M. Yoshikawa, JAERI Report M 4494 (1971)
- /28/ E.F. Johnson, Princeton Report MATT-901 (1972)
- /29/ F.H. Tenney, G. Levin, Proc. 7th Symposium on Fusion Technology, Grenoble 1975, p. 257
- /30/ R.G. Mills, International School of Fusion Reactor Technology, Erice/Sicily 1972; Princeton Report MATT-949 (1973)
- /31/ A.V. Georgievsky et al., Proc. 6th Symposium on Engineering Problems of Fusion Research, San Diego 1975, p. 583